Accepted by ApJL, August 9 2004
Preprint typeset using LaTeX style emulateapj v. 6/22/04

arXiv:astro-ph/0405436v2 9 Aug 2004

AN X-RAY JET FROM A WHITE DWARF – DETECTION OF THE COLLIMATED OUTFLOW FROM CH CYGNI WITH *CHANDRA*

Duncan K. Galloway
Center for Space Research, 37-626b, Massachusetts Institute of Technology, Cambridge, MA 02139

and

J. L. Sokoloski*
Smithsonian Astrophysical Observatory, 60 Garden St., Cambridge, MA 02138

Accepted by ApJL, August 9 2004

ABSTRACT

Most symbiotic stars consist of a white dwarf accreting material from the wind of a red giant. An increasing number of these objects have been found to produce jets. Analysis of archival *Chandra* data of the symbiotic system CH Cygni reveals faint extended emission to the south, aligned with the optical and radio jets seen in earlier *HST* and VLA observations. CH Cygni thus contains only the second known white dwarf with an X-ray jet, after R Aquarii. The X-rays from symbiotic-star jets appear to be produced when jet material is shock-heated following collision with surrounding gas, as with the outflows from some protostellar objects and bipolar planetary nebulae.

Subject headings: binaries: symbiotic — stars: individual (CH Cygni) — stars: winds, outflows — white dwarfs — X-rays: general

1. INTRODUCTION

Collimated jets are produced by many accreting astrophysical systems, ranging from proto-stars, through stellar-mass black holes in X-ray binaries, to active galactic nuclei. Symbiotic stars, in which a white dwarf (WD) accretes from the wind of a red giant, are probably the most recently recognized class of jet-producing objects. There are currently at least 10-12 symbiotics with evidence for bipolar outflows (Brocksopp et al. 2004; Corradi et al. 2001). Very little is known about the X-ray properties of symbiotic-star jets, as only one symbiotic jet has been reported in the X-rays (R Aquarii; see Kellogg et al. 2001).

CH Cygni ($l = 81\overset{\circ}{.}86$, $b = +15\overset{\circ}{.}58$) is one of the best-studied symbiotic systems (for a review of CH Cyg's properties see Kenyon 2001). The multiple photometric and radial velocity periodicities present in the system suggest the possible presence of a third star (Hinkle et al. 1993). For the distance, we adopt 245 ± 50 pc, from the mode of the Hipparcos parallax probability distribution (Perryman et al. 1997). Evidence for a radio jet was first detected between April 1984 and May 1985, coincident with a strong radio outburst and a substantial decline in the visual magnitude (Taylor et al. 1986). Subsequent radio and optical observations confirmed the extended emission as arising from a jet (Crocker et al. 2001), and also revealed that the jet position angle on the sky changes with time, suggesting that the jet axis precesses with a period of ≈ 6520 d (Crocker et al. 2002). Changes in the fast optical flickering in 1997, after a jet was produced, have also suggested a direct connection between the accretion disk and jet production in CH Cyg (Sokoloski & Kenyon 2003a). X-ray emission was first conclusively detected from CH Cyg by *EXOSAT* on 1985 May 24, at a flux of 1.3×10^{-11} ergs cm^{-2} s^{-1} (0.02–2.5 keV; Leahy & Taylor 1987). Subsequent *ASCA* observations revealed a complex X-ray spectrum which could be fit either with multiple thermal components (Ezuka et al. 1998) or a single-temperature thermal spectrum attenuated by an ionized absorber (Wheatley 2001).

Here we describe analysis of a *Chandra* observation in which we detect, for the first time, the X-ray jet in CH Cyg.

2. OBSERVATIONS

We analyzed an observation of CH Cyg acquired between 2001 March 27 06:22 and 20:02 UT, by the *Chandra X-ray Observatory* (Weisskopf et al. 2002). The observation was made in timed/FAINT mode with the high-energy transmission grating (HETG) in place, although the source flux was too low to obtain a high signal-to-noise grating spectrum (the first-order count rate was 6.3×10^{-3} count s^{-1}). Thus, we did not consider the dispersed spectra for our analysis. The CCDs are sensitive to photons in the 0.2–10 keV energy range, and have a pixel size of $0\overset{''}{.}492$. The zeroth-order image fell on the S3 (backside-illuminated) chip of the ACIS-S array. The standard data filtering resulted in a net exposure time of 47.082 ks. To analyze these archival data, we used CIAO[1] software version 3.0.2 and the *Chandra* calibration database version 2.26.

3. RESULTS

CH Cyg was detected with a total zeroth order count rate of 1.95×10^{-2} count s^{-1}. The image was not affected by pile-up. The centroid position was R.A. $= 19^{\rm h}24^{\rm m}33\overset{\rm s}{.}076$, decl. $= +50^\circ14'29\overset{''}{.}21$ (J2000.0), which agrees to within $0\overset{''}{.}11$ with the *Hipparcos* position of the optical counterpart HD 182917 (Perryman et al. 1997). This offset is well within *Chandra*'s 90% pointing accuracy[2] of $0\overset{''}{.}6$. The binned

Electronic address: duncan@space.mit.edu
*NSF Astronomy and Astrophysics Fellow.
Electronic address: jsokolos@cfa.harvard.edu

[1] See http://cxc.harvard.edu/ciao
[2] See http://cxc.harvard.edu/cal/ASPECT/celmon

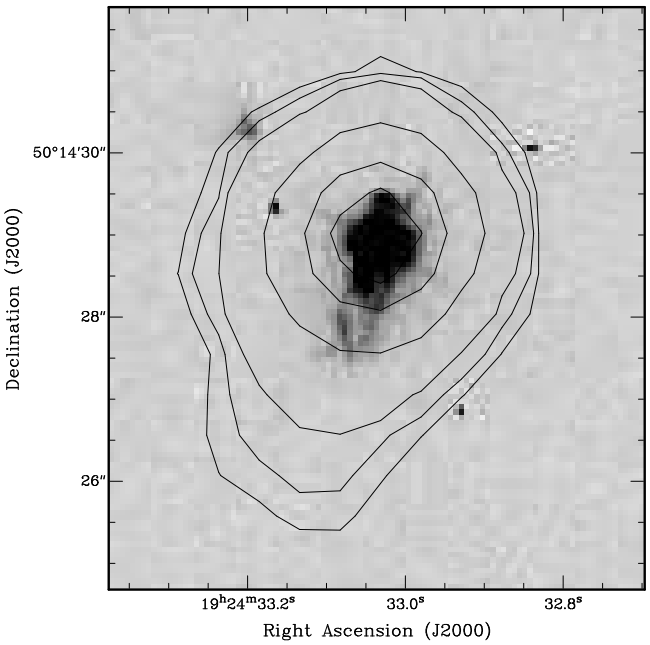

FIG. 1.— *Chandra* & *HST* images of the jet in CH Cyg. The contours show the zeroth order *Chandra* image from the 2001 March 27 observation, after smoothing with a Gaussian filter of radius 1". The contour values are 0.73, 1.2, 2, 10, 30, 50 and 90 counts per pixel. The greyscale shows the *HST* WFPC2 image from 1999 August 12 in the O III 495.9 nm & 500.7 nm filter (i.e. filter F502N); these data are also shown in Fig. 4c of Eyres et al. (2002).

zeroth order image of CH Cyg is shown in Fig. 1.

The source exhibited a faint extension ~ 2–$4''$ to the south-southeast. At the source position, $38\farcs1$ from the optical axis, no significant deviations from the optimal point-spread function (PSF) are expected (the 80% encircled energy radius for an on-axis point source is $0\farcs685$ at ≈ 1 keV). At the satellite roll angle used, the readout axis was perpendicular to the observed extension. To verify the source extension, we generated a simulated point-spread function (PSF) with the *Chandra* Ray-Tracer (ChaRT[3]) in combination with the Model of AXAF Response to X-rays (MARX[4]) simulation software, using the zeroth-order spectrum (see below) as input. We measured the radial surface brightness profile of the simulated zeroth-order image, and the resulting point-spread function is shown as a grey ribbon in Fig. 2. We also measured the observed radial profile of CH Cyg, both in the southern region where the source is extended, and over the rest of the image excluding this region (see Fig. 1). The extension we observed in the binned zeroth-order image (Fig. 1) is apparent as an excess above the radial surface brightness profiles of both the simulated image and the non-southern directions of the observed images.

We extracted 43 photons from the extended southern region, excluding photons within $1\farcs72$ of the centroid position. The probability of observing this many photons, given the extent of the simulated point source and assuming Poisson statistics, is 1.67×10^{-13}, corresponding to a significance of 7.4σ. The position angle of the extended emission (measured anticlockwise through east from north) of the principal component of the photon distribution was 164°, consistent with contemporary measurements of the CH Cyg jet from VLA/MERLIN radio and HST optical measurements (Crocker et al. 2002). We therefore conclude that the extension observed in the *Chandra* image is due to X-ray emission from the jet in CH Cyg. The northern optical jet is too small to be resolved with *Chandra*, and we see no evidence for extended emission in that direction.

The hardness ratio (calculated from the total counts > 2 keV divided by the counts < 2 keV), indicates that the extended emission (hardness ratio 0.65) was significantly softer than the central source (1.69). The photon distribution was, however, qualitatively similar to that of the zeroth-order image, with peaks below 1 keV and around 5 keV (Fig. 3). To characterize the jet spectrum, we fit the data with an absorbed, $0.18^{+0.06}_{-0.07}$ keV Raymond-Smith (RS) component for the emission < 2 keV and a broad ($\sigma \approx 1$ keV) Gaussian at $5.6^{+0.6}_{-0.5}$ keV (1σ errors) for the emission > 2 keV, each with a neutral interstellar absorbing column density fixed at 7×10^{20} cm^{-2} (from the HI survey of Stark et al. 1992). We found an acceptable fit with a C-statistic (appropriate for low-count per bin regimes; Cash 1979) of 4.0, below which fell only 6% of 1000 Monte-Carlo simulated spectra. Extrapolating this model beyond the *Chandra* energy limits, we estimate an unabsorbed bolometric flux of 1.2×10^{-13} ergs cm^{-2} s^{-1}, giving a jet luminosity of 9×10^{29} ergs s^{-1}.

We also fit the total zeroth-order spectrum, taking photons from within a circle of radius $\approx 5''$ around the centroid position. We used photons from an annulus 5–$10''$ from the centroid position as background. The spectrum exhibited two broad peaks, around 1 and 5 keV, as well as a narrow 6.64 keV line (Fig. 3), similar to the earlier ASCA observation (Ezuka et al. 1998).

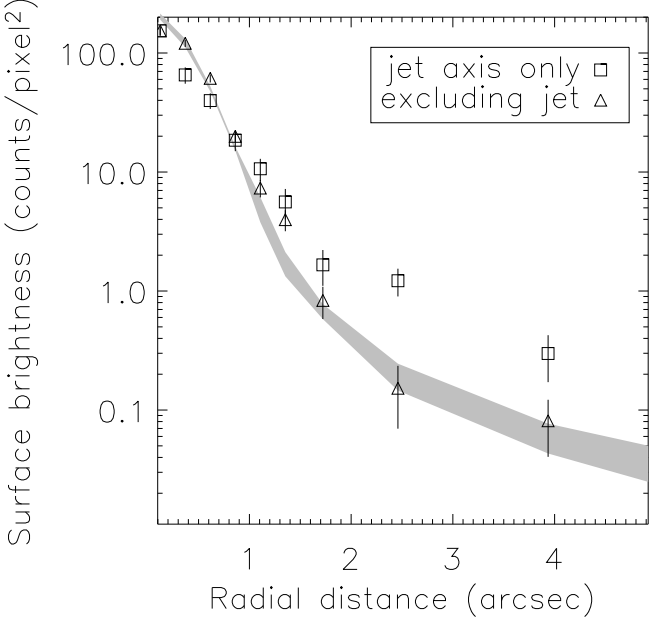

FIG. 2.— Radial surface brightness profiles of the zeroth-order *Chandra* image of CH Cyg. The grey ribbon shows the $\pm1\sigma$ limits on the simulated PSF from ChaRT/MARX, while the triangles show the radial profiles calculated using annulae excluding the southern extension. The squares show the radial profile for the southern extension. Error bars indicate the 1σ uncertainties.

[3] See http://cxc.harvard.edu/chart
[4] See http://space.mit.edu/CXC/MARX

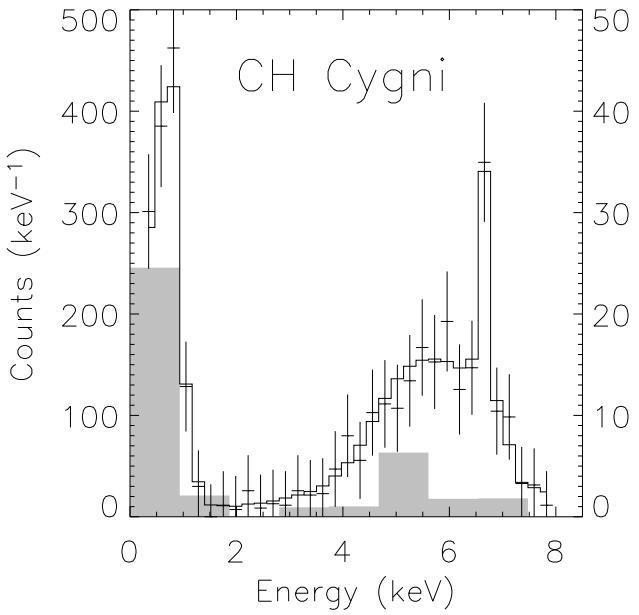

FIG. 3.— *Chandra* spectra from CH Cyg. The zeroth-order spectrum is shown as crosses, with error bars indicating the 1σ uncertainties. The dip in emission between 1–4 keV is not solely a consequence of a decreased effective area in that region. The histogram shows the best-fit model, consisting of 3 Raymond-Smith plasma components and a Gaussian to fit the line emission at 6.64 keV. The grey histgram shows the jet spectrum, scaled by a factor of 10 relative to the zeroth-order spectrum (right-hand y-axis).

Following those authors, we fit the net spectrum with a three-temperature RS plasma model plus a Gaussian to describe the 6.64 keV line. We obtained a C-statistic of 35.2. 53% of 1000 Monte-Carlo spectral simulations gave a lower value, indicating a statistically acceptable fit. The spectral parameters were roughly consistent with the ASCA values. By extrapolating this plasma-model spectrum beyond the *Chandra* energy limits, we derive an intrinsic (neglecting line-of-sight absorption) bolometric flux of 1.3×10^{-11} ergs cm^{-2} s^{-1}, giving a luminosity of 9.3×10^{31} ergs s^{-1} (for a distance of 245 pc). This luminosity is more than an order of magnitude smaller than typical values from earlier X-ray measurements of CH Cyg (e.g. Ezuka et al. 1998).

4. DISCUSSION

4.1. *The X-ray Jet in CH Cygni*

The extended X-ray emission in CH Cyg can be naturally explained by the collision of a collimated outflow of material with surrounding nebular gas. Outflow velocities for CH Cyg have been estimated as 600–2000 km s^{-1} and 1100 km s^{-1} in 1984/1985 (Taylor et al. 1986 and references therein, and Crocker et al. 2001 respectively), and > 1100 km s^{-1} in 1998-2000 (Eyres et al. 2002). For a typical outflow velocity of ~ 1300 km s^{-1}, the Rankine-Hugoniot jump conditions give $v_s = (4/3)v_{\rm flow} \approx 1700$ km s^{-1} (where v_s is the shock velocity and $v_{\rm flow}$ is the flow speed in the jet) for a strong shock. The temperature behind the shock, $T_{\rm ps}$, would then be

$$T_{\rm ps} = \frac{3}{16}\frac{\mu m_p}{k_B} v_s^2 = 4 \times 10^7 \left(\frac{v_s}{1700 \text{ km s}^{-1}}\right)^2 \left(\frac{\mu}{0.6}\right) \text{ K}, \quad (1)$$

where μ is the mean molecular weight, k_B is Boltzmann's constant, m_P is the proton mass, and we have assumed that the gas is ideal. A plasma with a post-shock temperature of 4×10^7 K produces X-rays in the 4-5 keV range; although we have insufficient jet X-ray photons to perform formal spectral fitting, we detect X-ray-jet photons at these energies. The data are thus consistent with material heated in a strong shock.

Softer X-ray photons are also detected from the jet. The time scale for hot plasma to adiabatically cool by flowing out from behind the shock is given roughly by the width of the jet divided by the sound speed. For the jet parameters of CH Cyg, this time is a few months. Thus, the lower-temperature jet emission (photons around 1 keV) could be due to material that has expanded perpendicular to the flow of the jet. Alternatively, a range of temperatures could arise from multiple shocks in the jet.

Adopting $v_s = 1700$km s^{-1} and a jet size of $4''$ on 2001 March 27, we can estimate the epoch of jet production. For $d = 245$ pc, we derive a mean proper motion for the jet of $1''.46$ yr^{-1}. The extended *Chandra* emission is therefore consistent with having been produced by material that was ejected in mid-1998. At that time, CH Cyg underwent a transition into an optical high state (see e.g. Crocker et al. 2001; Eyres et al. 2002; Sokoloski & Kenyon 2003b). The detection of extended radio emission in 1995 by Crocker et al. (2001) suggests that a

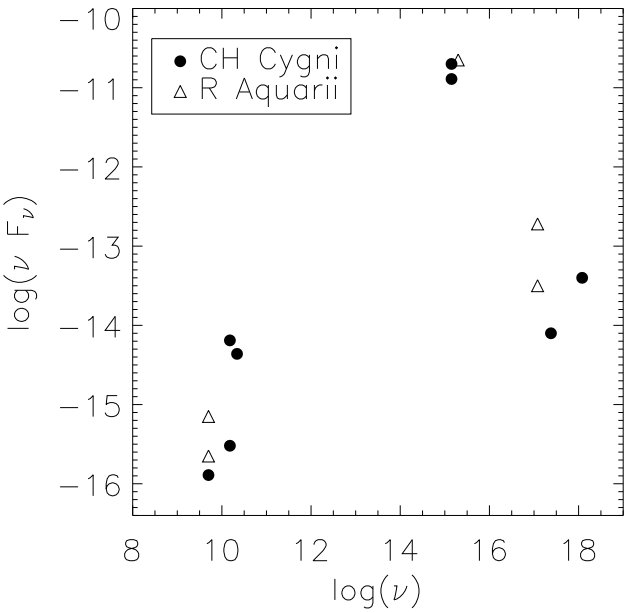

FIG. 4.— Comparison of the approximate spectral energy distributions for the jet emission from CH Cyg (filled circles) and R Aqr (open triangles). The radio data for CH Cyg are from Crocker et al. (2001) and Karovska et al. (1998), and for R Aqr are from Dougherty et al. (1995), Lehto & Johnson (1992) and Kafatos et al. (1989). The UV data for CH Cyg are from Eyres et al. (2002), and for R Aqr are from Contini & Formiggini (2003). The X-ray measurements for CH Cyg are from this work, and for R Aqr are from Kellogg et al. (2001). The UV fluxes for CH Cyg are not extinction corrected, and it is not known whether the UV flux for R Aqr from Contini & Formiggini (2003) is extinction corrected. The CH Cyg jet X-ray fluxes are absorption corrected using the Galactic column only.

jet ejection also occurred in association with a transition to the optical high state in 1992. The other two jet ejections, in 1984/85 (Taylor et al. 1986) and 1997 (Karovska et al. 1998), were associated with transitions from high to low optical states. Thus there appear to be at least two different scenarios in which jets can be produced in CH Cyg. This situation is reminiscent of X-ray binaries, which can produce discrete ejections in association with X-ray state changes, possibly in response to an extreme physical change in the accretion flow (Fender & Hendry 2000).

4.2. *Non-relativistic X-ray Jets*

The only other symbiotic star currently known to have an X-ray jet is R Aqr (see Kellogg et al. 2001). Compared to CH Cyg the R Aqr jet is both more extended on the sky ($30''$ for the R Aqr southern jet compared to $4''$ for CH Cyg) and physically larger (roughly 6000 AU compared to roughly 1000 AU for CH Cyg). Although the measured jet fluxes for the two sources are comparable, Kellogg et al. (2001) found that few of the jet X-ray photons from R Aqr had energies greater than 1 keV. The R Aqr jet spectrum revealed emission lines at 400 and 550 eV and was generally consistent with a shocked plasma out of ionization equilibrium (the plasma temperatures for the northeastern and southwestern jets were found to be 2×10^7 K and 2×10^6 K respectively). A follow-up *Chandra* observation of R Aqr revealed that the northern R Aqr X-ray jet is expanding at a velocity of $\approx$ 600 $\mathrm{km\,s^{-1}}$ (E. Kellogg, private communication). Contini & Formiggini (2003) compiled and modeled the full spectral energy distribution (SED) of R Aqr, and found that the jet emission is due to a combination of photoionization and shock heating. In units of νF_ν, where ν is radiation frequency and F_ν is flux density, the R Aqr jet emission is strongest in the UV, weakest in the radio, and in between for the X-rays. In Fig. 4 we plot both the SED data compiled for R Aqr by Contini & Formiggini (2003) and that for CH Cyg obtained from the literature and our work in the X-rays. The jet SEDs for R Aqr and CH Cyg are quite similar, despite R Aqr appearing to have a slower shock speed, slightly lower post-shock temperatures, and a larger size. This similarity suggests that other symbiotic-star jets might also be expected to emit X-rays.

In addition to symbiotic-star jets, two other types of non-relativistic jet have been detected in the X-rays: protostellar jets (in Herbig-Haro objects) and collimated outflows from the central stars or binaries in planetary nebulae (PNe). In both cases, the X-rays also appear to be due to shock heating as the outflowing material collides with surrounding gas. In the two known X-ray-bright protostellar outflows (HH2, Pravdo et al. 2001; and YL1551 IRS5 = HH 154, Favata et al. 2002), the jet X-ray luminosities are a few times 10^{29} ergs (similar to CH Cyg and R Aqr) and the jet plasma temperatures are $\sim 10^6$ K. Soker & Kastner (2003) summarized six observations of PNe by *Chandra* and *XMM-Newton*, four of which revealed diffuse X-ray emission with temperatures of a few time 10^6 K. These four PNe all show evidence for high-velocity, collimated flows (Kastner et al. 2003). Soker & Kastner (2003) suggest that a hidden binary companion within each of these PNe accrete from the AGB-star wind and produce an X-ray jet. They note that the X-ray production mechanism would thus be similar to that in the protostellar outflows mentioned above, and the symbiotic star R Aqr. In fact, an additional PNe with X-ray-jet emission, Menzel 3, is known to contain a symbiotic pair at its center (Kastner et al. 2003; Zhang & Liu 2002; Schmeja & Kimeswenger 2001). The links between the X-ray jets in symbiotic stars, protostellar outflows, and PNe are thus quite compelling.

We thank J. Lazendic for help generating and overlaying the images, as well as J. Raymond and S. Kenyon for useful discussion. We also thank the referee, M. Bode, for his helpful suggestions. This work was funded in part by the NASA Long Term Space Astrophysics program under grant NAG 5-9184 (PI: Chakrabarty). JLS is supported by an NSF Astronomy and Astrophysics Postdoctoral Fellowship under award AST-0302055. This research has made use of data obtained through the High Energy Astrophysics Science Archive Research Center Online Service, provided by the NASA/Goddard Space Flight Center.

REFERENCES

Brocksopp, C., Sokoloski, J. L., Kaiser, C., Richards, A. M., Muxlow, T. W. B., & Seymour, N. 2004, MNRAS, 347, 430
Cash, W. 1979, ApJ, 228, 939
Contini, M. & Formiggini, L. 2003, MNRAS, 339, 148
Corradi, R. L. M., Munari, U., Livio, M., Mampaso, A., Gonçalves, D. R., & Schwarz, H. E. 2001, ApJ, 560, 912
Crocker, M. M., Davis, R. J., Eyres, S. P. S., Bode, M. F., Taylor, A. R., Skopal, A., & Kenny, H. T. 2001, MNRAS, 326, 781
Crocker, M. M., Davis, R. J., Spencer, R. E., Eyres, S. P. S., Bode, M. F., & Skopal, A. 2002, MNRAS, 335, 1100
Dougherty, S. M., Bode, M. F., Lloyd, H. M., Davis, R. J., & Eyres, S. P. 1995, MNRAS, 272, 843
Eyres, S. P. S., Bode, M. F., Skopal, A., Crocker, M. M., Davis, R. J., Taylor, A. R., Teodorani, M., Errico, L., Vittone, A. A., & Elkin, V. G. 2002, MNRAS, 335, 526
Ezuka, H., Ishida, M., & Makino, F. 1998, ApJ, 499, 388
Favata, F., Fridlund, C. V. M., Micela, G., Sciortino, S., & Kaas, A. A. 2002, A&A, 386, 204
Fender, R. & Hendry, M. 2000, MNRAS, 317 (1), 1
Hinkle, K. H., Fekel, F. C., Johnson, D. S., & Scharlach, W. W. G. 1993, AJ, 105, 1074
Kafatos, M., Hollis, J. M., Yusef-Zadeh, F., Michalitsianos, A. G., & Elitzur, M. 1989, ApJ, 346, 991
Karovska, M., Carilli, C. L., & Mattei, J. A. 1998, Journal of the American Association of Variable Star Observers (JAAVSO), 26, 97
Kastner, J. H., Balick, B., Blackman, E. G., Frank, A., Soker, N., Vrtílek, S. D., & Li, J. 2003, ApJ, 591, L37
Kellogg, E., Pedelty, J. A., & Lyon, R. G. 2001, ApJ, 563, L151
Kenyon, S. J. 2001, in Encyclopedia of Astronomy and Astrophysics, ed. P. Murdin (London: Institute of Physics)
Leahy, D. A. & Taylor, A. R. 1987, A&A, 176, 262
Lehto, H. J. & Johnson, D. R. H. 1992, Nature, 355, 705
Perryman, M. A. C., Lindegren, L., Kovalevsky, J., Hoeg, E., Bastian, U., Bernacca, P. L., Crézé, M., Donati, F., Grenon, M., van Leeuwen, F., van der Marel, H., Mignard, F., Murray, C. A., Le Poole, R. S., Schrijver, H., Turon, C., Arenou, F., Froeschlé, M., & Petersen, C. S. 1997, A&A, 323, L49
Pravdo, S. H., Feigelson, E. D., Garmire, G., Maeda, Y., Tsuboi, Y., & Bally, J. 2001, Nature, 413, 708
Schmeja, S. & Kimeswenger, S. 2001, A&A, 377, L18
Skopal, A., Bode, M. F., Lloyd, H. M., & Tamura, S. 1996, A&A, 308, L9

Soker, N. & Kastner, J. H. 2003, ApJ, 583, 368
Sokoloski, J. L. & Kenyon, S. J. 2003a, ApJ, 584, 1021
—. 2003b, ApJ, 584, 1027
Stark, A. A., Gammie, C. F., Wilson, R. W., Bally, J., Linke, R. A., Heiles, C., & Hurwitz, M. 1992, ApJS, 79, 77
Taylor, A. R., Seaquist, E. R., & Mattei, J. A. 1986, Nature, 319, 38
Weisskopf, M. C., Brinkman, B., Canizares, C., Garmire, G., Murray, S., & Van Speybroeck, L. P. 2002, PASP, 114, 1
Wheatley, P. J. 2001, in AIP Conf. Proc. 599: X-ray Astronomy: Stellar Endpoints, AGN, and the Diffuse X-ray Background, 1007–1010
Zhang, Y. & Liu, X.-W. 2002, MNRAS, 337, 499